Universiteit
Leiden
The Netherlands

Control of early plant development by light quality

Spaninks, K.

Citation
Spaninks, K. (2023, May 10). *Control of early plant development by light quality*. Retrieved from https://hdl.handle.net/1887/3618264

Version:	Publisher's Version
License:	Licence agreement concerning inclusion of doctoral thesis in the Institutional Repository of the University of Leiden
Downloaded from:	https://hdl.handle.net/1887/3618264

Note: To cite this publication please use the final published version (if applicable).

Chapter 2

Local phytochrome signalling limits root growth in light by repressing auxin biosynthesis.

Kiki Spaninks[1] and Remko Offringa[1]

[1]Plant Developmental Genetics, Institute of Biology Leiden, Leiden University, Sylviusweg 72, 2333 BE, Leiden, Netherlands.

Abstract

In nature, plant shoots are exposed to light whereas the roots grow in darkness. Surprisingly, many root studies rely on *in vitro* systems that leave the roots exposed to light whilst ignoring the possible effects of this light on root development. Here, we investigated how direct root illumination affects root growth and development in Arabidopsis and tomato. Our results show that in light-grown Arabidopsis roots activation of local phytochrome A and B by far-red or red light inhibits respectively PHYTOCHROME INTERACTING FACTORs 1 or 4, resulting in decreased *YUCCA4* and *YUCCA6* expression. As a result, the auxin levels in the root apex become suboptimal, ultimately resulting in reduced growth of light-grown roots. These findings highlight once more the importance of using *in vitro* systems where roots are grown in darkness, for studies that focus on root system architecture. Moreover, we show that the response and components of this mechanism are conserved in tomato roots, thus signifying its importance for horticulture as well. Our findings open up new research possibilities to investigate the importance of light-induced root growth inhibition for plant development, possibly by exploring putative correlations with responses to other abiotic signals, such as temperature, gravity, touch, or salt stress.

Keywords: Root growth, PHY signalling, Auxin biosynthesis, Arabidopsis, tomato

Introduction

Light is an essential energy source for life on earth. Aside from driving photosynthesis in cyanobacteria and plants, light also acts as an environmental cue that regulates almost all aspects of plant growth and development. Perception of light by photoreceptors initiates a variety of physiological responses that are collectively referred to as photomorphogenesis (Arsovski et al., 2012). The blue light photoreceptor families of cryptochromes, phototropins and Zeitlupes act together with the red (R) / far-red (FR)-sensitive family of phytochromes (PHYs) to regulate developmental processes ranging from germination to flowering, often by influencing hormonal pathways (de Wit et al., 2016). Generally, only the plant shoot is considered when light perception is discussed, as in nature, plant roots grow in darkness. However, root morphology and development are greatly influenced by light (Lee et al., 2017). Photoreceptors regulate root development either by detecting light in the shoot and inducing transmission of mobile signalling molecules, or by perceiving direct or stem-piped light in the roots (Lejay et al., 2008; Sassi et al., 2012; Chen et al., 2016; Lee et al., 2016). A healthy root system is vital for plants for the absorption of water and nutrients, for mechanical support, and as a sink organ (Petricka et al., 2012). Root-localised light perception is physiologically relevant when growing plants *in vitro* or in aeroponic systems. Therefore, elucidation of the local light perception and signalling pathways in the roots is particularly important for studies that focus on root system architecture (RSA), and that have been conducted in *in vitro* systems where the plant roots are exposed to light. Excluding the effect of light, while using light-grown root (LGR) systems in these studies, might result in inadequate

predictive models for RSA phenotypes. For example, an immediate and strong outburst of reactive oxygen species (ROS) has been observed in roots grown in LGR conditions, which might influence the overall RSA (Yokawa et al., 2011). To avoid such stresses, and their adverse effects on the RSA, a dark-grown root (DGR) system, such as the D-root system, should be used for future RSA studies (Silva-Navas et al., 2015). Also in horticulture, where plants are often grown in aeroponic systems or on light-transmittable substrates, such as glass wool, the unintended LGR conditions may influence the growth and development of crop plants. Although crop breeding programs mainly focus on shoot-related phenotypes, changes in RSA might improve crop tolerance to a range of abiotic stresses including drought, salinity, and nutrient limitations (Koevoets et al., 2016).

Here we show that when *Arabidopsis thaliana* (Arabidopsis) seedlings are grown in the DGR condition, the bHLH transcription factors PHYTOCHROME INTERACTING FACTOR 1 (PIF1) and PIF4 promote local auxin biosynthesis through upregulation of *YUCCA4* (*YUC4*) and *YUC6* genes, which results in close-to-optimal auxin levels in the RAM, and thus in normal root development. However, in the LGR condition, FR or R light activation of respectively PHYA and PHYB triggers the targeted degradation of these PIFs, resulting in reduced expression of *YUC4* and *YUC6*, and ultimately in shorter roots due to suboptimal auxin levels in the RAM. In addition to the identification of this molecular mechanism, we show that the LGR response and components of this pathway are conserved between Arabidopsis and the horticultural crop tomato (*Solanum lycopersicum*).

Results

Cell growth in the proximal root meristem is decreased in light-grown roots.

Arabidopsis seedlings of ecotypes Columbia (Col-0) and Landsberg *erecta* (L*er*) were grown in the LGR or DGR condition for seven days. Seedlings of both ecotypes showed significantly shorter roots in the LGR condition compared to the DGR condition (**Figures 1A, B**). These results were in line with previously published data using the D-root system (Silva-Navas et al., 2015). Interestingly, hypocotyls of LGR seedlings were also significantly shorter than those of DGR seedlings (**Figures 1A, S2A**). However, since the shoot/root ratio of LGR seedlings was significantly higher than that of DGR seedlings (**Figure S2B**), we conclude that root growth inhibition in the LGR condition is independent of reduced hypocotyl growth. Root growth depends on the balance between cell proliferation and cell expansion in the RAM and on vast asymmetric cell expansion in the elongation zone. In general, a higher number of cortex cells in the proximal meristem of the root apex correlates with longer roots (Baskin, 2013). However, root length can also be determined by the size of these cortex cells (Aceves-García et al., 2016). Propidium iodide (PI) staining and imaging by confocal microscopy detected no significant differences in the number of cortex cells between root tips of LGR and DGR seedlings, whereas the proximal meristem size (in µm) was significantly smaller in LGR seedlings (**Figure 1C, D**). These data showed that direct illumination of roots results in a reduced cell growth in the proximal meristem of the root apex, ultimately leading to a shorter primary root.

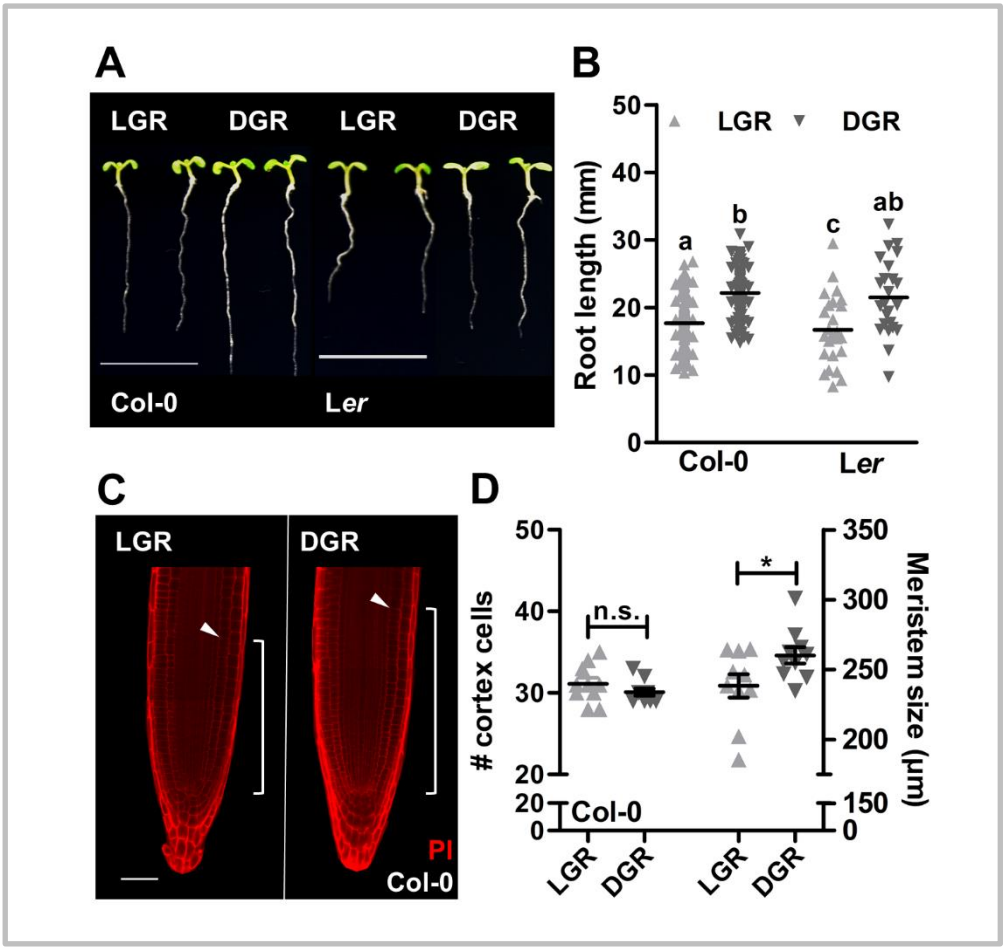

Reduced growth of light-grown roots correlates with a decrease in local auxin biosynthesis in the RAM.

As a key regulator of root growth and development, auxin might be the driving force behind cortex cell growth in the DGR condition. Confocal analysis of the *pDR5::GFP* auxin response reporter in Arabidopsis Col-0 seedlings showed a significant reduction of the GFP signal in the RAM of LGR seedlings,

Figure 1: Cell growth in the proximal meristem is decreased in light-grown roots.
A. Representative 7-day-old Arabidopsis seedlings of ecotypes Columbia (Col-0) and Landsberg *erecta* (L*er*) grown in the light-grown roots (LGR) or the dark-grown roots (DGR) condition. For presentation purposes, seedlings were transferred to black agarose plates before photographing. **B.** Quantification of the primary root length of 7-day-old Col-0 and L*er* seedlings grown in the LGR or DGR condition. **C.** Confocal images of Col-0 root tips that were stained with propidium iodide (PI). Arrowheads indicate the end of the proximal meristem and white brackets indicate the meristem size. **D.** Quantification of the proximal meristem size in number of cortex cells (left) or in µm (right) of Col-0 seedlings grown in the LGR or DGR condition. Primary root lengths in **B** were compared using a one-way ANOVA followed by a Tukey's test. Letters **a**, **b**, and **c** indicate statistically different values, $p<0.05$. The LGR condition in **D** was compared to the DGR condition using a two-sided Student's *t*-test (*$p<0.05$, n.s. = not significant). Scale bars indicate 1 cm in **A**, and 50 µm in **C**. In **B** (n=30) and **D** (n=20) the horizontal line indicates the mean, error bars represent standard error of the mean (for some not visible due to limited variation) and triangles indicate values of biologically independent observations. Similar results were obtained from three (**A-B**), or from two independent experiments (**C-D**).

compared to DGR seedlings (**Figures 2A, B**), suggesting that light inhibits the auxin response in the RAM. To investigate if reduced root growth in the LGR condition was caused by a decrease in auxin levels, wild-type Col-0 seedlings were grown on medium supplemented with 1-naphthaleneacetic acid (NAA) concentrations varying between 0 and 50 nanomolar. In LGR seedlings, NAA concentrations up to 40 nM maximised root growth, whereas addition of 50 nM NAA reduced root growth (**Figure 2C**). In contrast, for DGR seedlings the

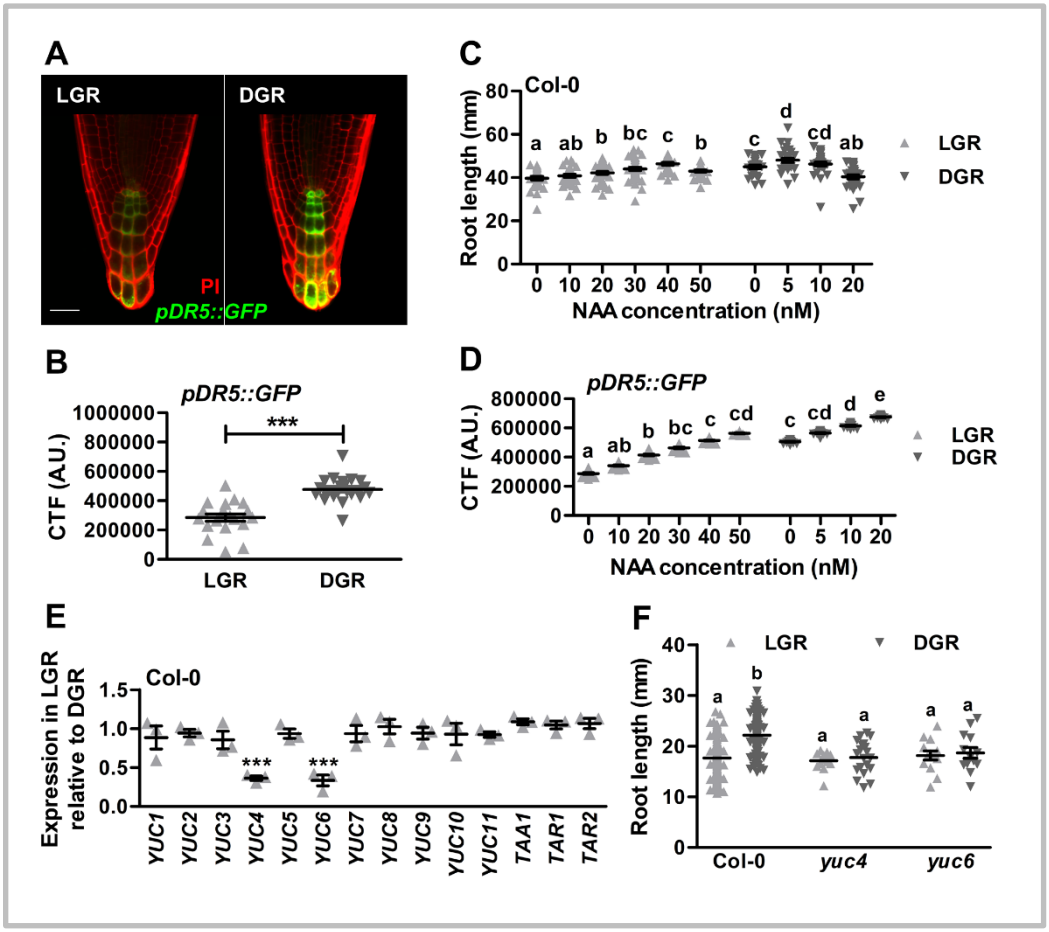

addition of 5 nM NAA maximised root growth, whereas 20 nM NAA resulted in clear root growth inhibition. The 8-fold increase in NAA concentration for optimal root growth of LGR seedlings was in line with the reduced *DR5::GFP* expression. NAA treatment of LGR- and DGR-grown *pDR5::GFP* seedlings confirmed that reporter gene expression increased with increasing NAA concentrations, and that expression in DGR RAMs was always significantly higher compared to LGR RAMs (**Figure 2D**), and thus that reduced primary root growth in the LGR condition was caused by the reduced auxin response

Figure 2: Growth inhibition of roots by light is caused by a decrease in local auxin biosynthesis in the RAM.
A. Confocal images of the root apical meristem (RAM) of 7-day-old *pDR5::GFP* (green signal) seedlings grown in the LGR or the DGR condition. The roots were stained with propidium iodide (PI, red signal). **B.** Quantification of the corrected total fluorescence (CTF) of the RAM. **C-D.** Quantification of the primary root length of Col-0 seedlings (**C**) and the CTF of *pDR5::GFP* seedlings (**D**) grown in the LGR or DGR condition on medium containing different concentrations of 1-naphthaleneacetic acid (NAA). **E.** Quantitative RT-PCR analysis of *YUC1-11*, *TAA1*, *TAR1* and *TAR2* expression in the RAM of 7-day-old Col-0 seedlings that were grown in the LGR condition, relative to gene expression levels of seedlings grown in the DGR condition. **F.** Quantification of the primary root length of 7-day-old Col-0, *yuc4* and *yuc6* seedlings grown in the LGR or DGR condition. In **B** and **E**, the LGR condition was compared to the DGR condition using a two-sided Student's *t*-test (***$p<0.001$). In **C**, **D** and **F**, NAA concentrations and primary root lengths were compared using a one-way ANOVA followed by a Tukey's test. Letters **a**, **b**, **c**, **d**, and **e** indicate statistically different values, $p<0.05$. The scale bar indicates 50 µm in **A**. In **B** (n=20), **C**, **D**, **F** (n=30) and **E** (n=3), the horizontal line indicates the mean, error bars represent standard error of the mean (for some not visible due to limited variation) and triangles indicate values of biologically independent observations. Similar results were obtained from two (**A-B**), or from three independent experiments (**C-F**).

in the RAM. For both conditions, there was a strong positive correlation between increase in GFP signal and increasing NAA concentrations. This correlation was linear with a statistically indistinguishable regression coefficient *b* (**Table S1**), indicating that the reduced auxin response in LGR RAMs was caused by lower endogenous auxin levels, rather than a reduced auxin responsiveness. It is therefore most likely that either auxin biosynthesis or transport is affected in LGR seedlings, resulting in a reduced auxin response

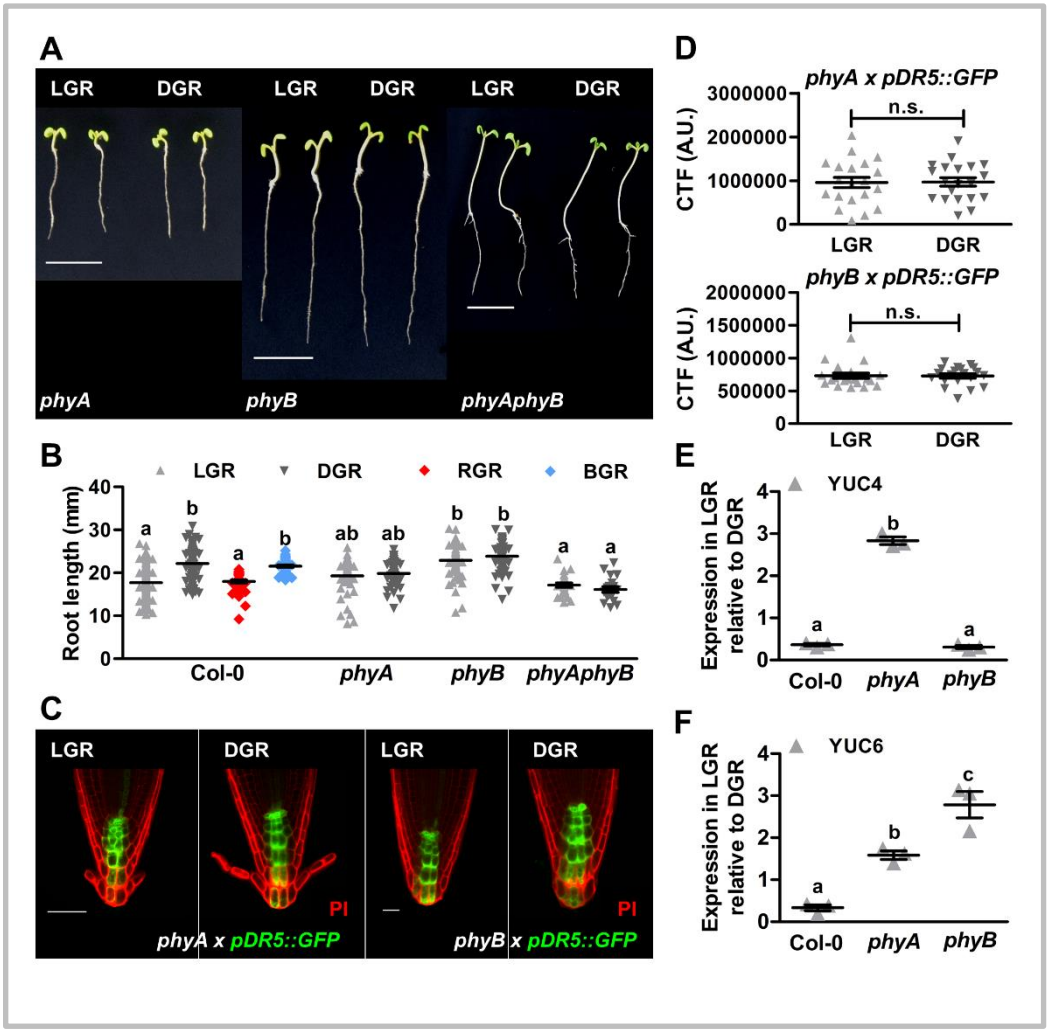

in the RAM. Expression analysis of the auxin biosynthesis genes *YUC1-11*, *TAA1*, *TAR1* and *TAR2* in LGR or DGR RAMs by qRT-PCR showed that *YUC4* and *YUC6* expression was significantly lower in LGR compared to DGR seedlings (**Figure 2E**). Moreover, the dark-induced enhancement of root growth was lost in *yuc4* and *yuc6* mutant seedlings grown in the DGR condition (**Figure 2F**). In contrast, mutants of important auxin influx and

Figure 3: PHYA and PHYB trigger root growth inhibition in response to light.

A. Representative 7-day-old *phy* mutant seedlings grown in the LGR or the DGR condition. For presentation purposes, seedlings were transferred to black agarose plates before photographing. **B.** Quantification of the primary root length of 7-day-old Col-0 seedlings grown in the LGR, DGR, red light-grown roots (RGR) or blue light-grown roots (BGR) condition, and *phy* seedlings grown in the LGR or DGR condition. **C.** Confocal images of the root apical meristem (RAM) of *phyA x pDR5::GFP* and *phyB x pDR5::GFP* (green signal) seedlings grown in the LGR or DGR condition. Root tips were stained with propidium iodide (PI, red signal). **D.** Quantification of the corrected total fluorescence (CTF) of the RAM of *phyA x pDR5::GFP* and *phyB x pDR5::GFP* seedlings. **E-F.** Quantitative RT-PCR analysis of *YUC4* (**E**) and *YUC6* (**F**) expression in the RAM of 7-day-old Col-0, *phyA* and *phyB* seedlings that were grown in the LGR condition, relative to gene expression levels in the RAM of seedlings grown in the DGR condition. In **B**, **E** and **F**, primary root lengths and relative gene expression were compared using a one-way ANOVA followed by a Tukey's test. Letters **a**, **b** and **c** indicate statistically different values, $p<0.05$. The LGR condition in **D** was compared to the DGR condition using a two-sided Student's *t*-test (n.s. = not significant). Scale bars indicate 1 cm in **A**, and 50 µm in **C**. In **B** (n=30), **D** (n=20) and **E-F** (n=3), the horizontal line indicates the mean, error bars represent standard error of the mean (for some not visible due to limited variation) and triangles indicate values of biologically independent observations. Similar results were obtained from three (**A-B**, **E-F**), or from two independent experiments (**C-D**).

efflux carriers remained sensitive to the different light conditions, suggesting that auxin transport is not affected in LGR seedlings (**Figure S3A**). Altogether, these experiments indicated that lower *YUC4* and *YUC6* expression in the RAM of LGR seedlings causes a reduction in local auxin biosynthesis that ultimately leads to shorter roots.

Root-localised PHYA and PHYB mediate light-induced inhibition of root growth.

Since the differential auxin levels in LGR and DGR seedlings must be initiated by detection of light, we next investigated the LGR response in mutants of the three main photoreceptor families in land plants: the R/FR-inducible PHYs, and the blue light-induced cryptochromes (CRYs) and phototropins (PHOTs). Although their main functions might be above-ground, many photoreceptors of these families are also expressed in roots (Van Gelderen et al., 2018), and thus might be involved in root growth inhibition of LGR seedlings. For most of the single *phy*, *cry* and *phot* mutants, light-grown roots were significantly shorter

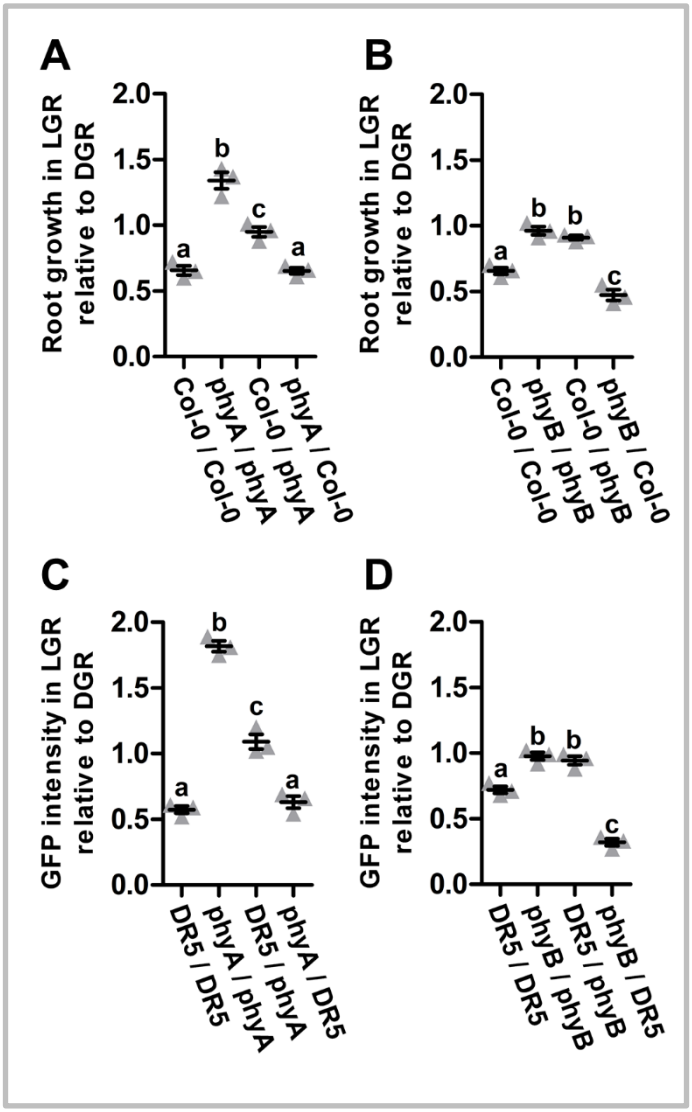

than dark-grown roots, indicating that the response of root growth to light was not affected (**Figure S3B**). For the *phyA* and *phyB* mutants, however, LGR and DGR roots were of the same length, suggesting that the sensitivity of the roots to light was lost in these mutants (**Figures 3A, B**). Moreover, analysis of the *phyAphyB* double mutant showed a similar loss of light sensitivity. Since PHYs are R/FR-responsive photoreceptors, we expected that only exposure of roots to spectra that contain R or FR wavelengths would result in root growth inhibition. To monitor root growth in response to different wavelengths, Arabidopsis seedlings were grown with their roots covered by clear (LGR), red (RGR) or blue (BGR) translucent plastic, or black paper covers (DGR). Primary root growth was significantly inhibited

Figure 4: Grafting: local PHYA and PHYB trigger root growth inhibition in response to light.

A-B. Quantification of the root growth of *phyA* and wild-type (Col-0) grafts (**A**), or *phyB* and Col-0 grafts (**B**) in the LGR condition, relative to the DGR condition, at 5 days post-grafting. **C-D**. Quantification of the corrected total fluorescence (CTF) of *pDR5::GFP* in the root apical meristem (RAM) of indicated grafts at 5 days post-grafting in the LGR relative to the DGR condition. Scion / rootstock combinations were grafted using 4-day-old *phyA* and Col-0 (**A**), *phyB* and Col-0 (**B**), *pDR5::GFP* and *phyA x pDR5::GFP* (**C**) or *pDR5::GFP* and *phyB x pDR5::GFP* (**D**) seedlings. Graft combinations were compared using a one-way ANOVA followed by a Tukey's test. Letters **a**, **b**, and **c** indicate statistically different values, $p<0.05$. In the graphs, the horizontal line indicates the mean, error bars represent standard error of the mean and triangles indicate values of biologically independent observations (n=5). Similar results were obtained from two independent experiments.

in LGR and RGR seedlings, but not in BGR or DGR seedlings (**Figure 3B**), confirming that inhibition of root growth is specific for R and FR light. The *pDR5::GFP* reporter showed a similar auxin response in the LGR and DGR condition in both the *phyA* and *phyB* mutant background (**Figures 3C, D**). In addition, quantitative RT-PCR analysis showed that expression of *YUC4* was significantly increased in the RAM of *phyA* seedlings grown in the LGR condition, compared to the DGR condition, whereas it was decreased in LGR Col-0 and *phyB* RAMs (**Figure 3E**). Moreover, *YUC6* was significantly increased in LGR *phyA* and *phyB* seedlings (**Figure 3F**). Together, this data suggests that inhibition of *YUC4* and *YUC6* expression by light is regulated by PHYA and partially by PHYB. Finally, to confirm that signalling through PHYA and PHYB is truly initiated in the root and not in the shoot, a series of grafting experiments were performed. The following scion / rootstock combinations were included: wild type / wild type (positive control), mutant / mutant (negative control), wild type / mutant (to study photoactivation in the shoot), and mutant / wild type (to study photoactivation in the root). As expected, the positive control grafts showed sensitivity to light, and the negative control grafts were insensitive. For both mutants, the grafts with wild-type roots retained light sensitivity, whereas the grafts with mutant roots had lost light sensitivity (**Figures 4A, B**), confirming that root-localised photoactivation of PHYA or PHYB initiates root growth inhibition by light. Finally, grafting of *phy x pDR5::GFP* seedlings with wild-type *pDR5::GFP* seedlings confirmed the correlation between primary root growth and auxin response in the RAM of grafted seedlings (**Figures 4C, D**). Altogether, the experiments described above showed that FR and R light directly activate root-localised PHYA and PHYB, respectively, to inhibit *YUC4* (PHYA) and *YUC6*

(PHYA and PHYB) expression, thus lowering local auxin levels to reduce primary root growth.

Light-activated root-localised phytochromes repress local auxin biosynthesis via PIF1 and PIF4.

Photoactivated PHYs can affect gene expression either through inhibition of ubiquitin E3 ligases, such as COP1/SPA, or by inhibition of the basic helix-loop-helix (bHLH) family of PIF transcription factors (Pham et al., 2018; Podolec and Ulm, 2018). Since PIF inhibition is exclusive for PHYA and PHYB signalling, we investigated PIFs as putative signalling components for root growth inhibition in LGR conditions. We selected PIF1 and PIF3, as they are targeted by both PHYA and PHYB, and the PHYB-exclusive target PIF4 for its known role in regulation of auxin biosynthesis (Franklin et al., 2011; Pham et al., 2018). Primary root growth measurements of *pif1*, *pif3* and *pif4* mutants grown in the LGR and DGR condition revealed that *pif1* and *pif4* seedlings were insensitive to root illumination, whereas *pif3* responded similar to wild-type seedlings (**Figures 5A, B**). In line with our results in *phyA* and *phyB* mutants, the *pDR5::GFP* response was the same in LGR and DGR conditions in *pif1* and *pif4* mutants (**Figures 5C, D**). Moreover, quantitative RT-PCR analysis showed a significant increase in *YUC4* in the RAM of light-grown *pif1* seedlings, compared to dark-grown seedlings, whereas LGR Col-0 and *pif4* RAMs showed a significant decrease (**Figure 5E**). Moreover, *YUC6* expression was significantly increased in the RAMs of LGR *pif1* and *pif4* but decreased in LGR Col-0 RAMs (**Figure 5F**). Since the *YUC4* and *YUC6* levels in *pif1* mutants were similar to those in *phyA* mutants (**Figure 3E, F**), PIF1 is most likely targeted by PHYA in response to FR light exposure of roots.

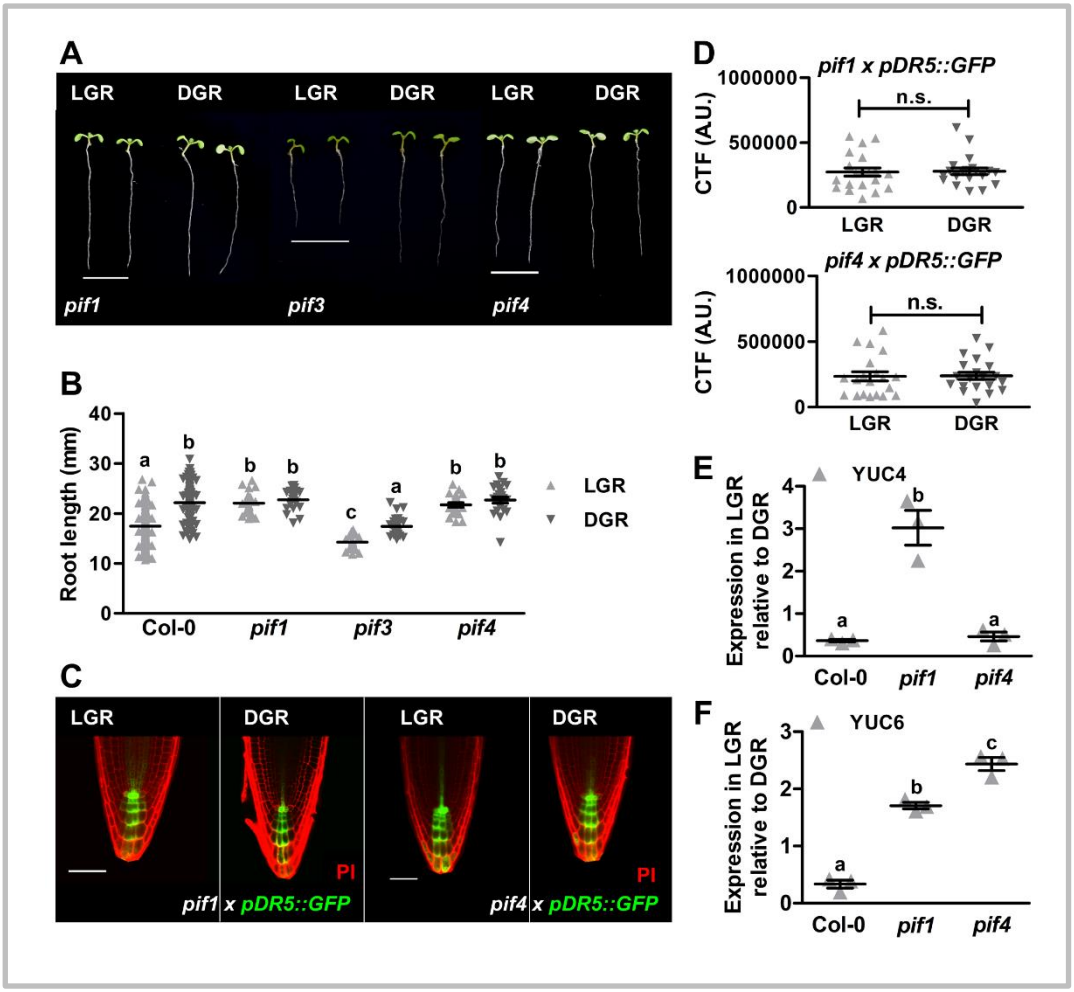

Likewise, the RAMs of LGR *pif4* mutants showed a significant decrease in *YUC4* expression and increase in *YUC6* expression, which was similar to *phyB* mutants (**Figure 3E, F**), suggesting that PHYB inhibits PIF4 in response to illumination of roots with R light.

Light-induced inhibition of root growth is partially conserved between Arabidopsis and tomato.

Figure 5: Light represses local auxin biosynthesis through PIF1 and PIF4.
A. Representative 7-day-old *pif* mutant seedlings grown in the LGR or the DGR condition. For presentation purposes, seedlings were transferred to black agarose plates before photographing. **B.** Quantification of the primary root length of 7-day-old Col-0 and *pif* seedlings grown in the LGR or DGR condition. **C.** Confocal images of the root apical meristem (RAM) of *pif1 x pDR5::GFP* and *pif4 x pDR5::GFP* (green signal) seedlings grown in the LGR or DGR condition. Root tips were stained with propidium iodide (PI, red signal). **D.** Quantification of the corrected total fluorescence (CTF) of *pDR5::GFP* in the RAM. **E-F.** Quantitative RT-PCR analysis of *YUC4* (**E**) and *YUC6* (**F**) expression in the RAM of 7-day-old Col-0, *pif1* and *pif4* seedlings grown in the LGR condition relative to the DGR condition. In **B**, **E** and **F**, primary root lengths were compared using a one-way ANOVA followed by a Tukey's test. Letters **a**, **b**, and **c** indicate statistically different values, $p<0.05$. In **D**, the LGR condition was compared to the DGR condition using a two-sided Student's *t*-test (n.s. = not significant). Scale bars indicate 1 cm in **A**, and 50 µm in **C**. In **B** (n=30), **D** (n=20) and **E-F** (n=3), the horizontal line indicates the mean, error bars represent standard error of the mean (for some not visible due to limited variation) and triangles indicate values of biologically independent observations. Similar results were obtained from three (**A-B**, **E-F**), or from two independent experiments (**C-D**).

The results described above clearly showed how the widely used LGR *in vitro* system results in suboptimal root growth in Arabidopsis. To investigate if the LGR condition can also lead to suboptimal root growth in horticulture, we included the economically important crop tomato in our experiments. Similar to Arabidopsis, wild-type tomato seedlings of both Moneymaker (MM) and the commercial hybrid Foundation (FO) showed a significant reduction in primary root growth in the LGR condition, compared to the DGR condition

(**Figures 6A, B**). Analysis of MM *phy* mutants in the LGR and DGR condition, showed that both *phyB2* single and *phyAphyB2* double mutant seedling roots were insensitive to light, whereas *phyB1* roots responded the same as wild-type roots. Interestingly, tomato *phyA* roots were significantly longer in the LGR condition, compared to the DGR condition, which is not the case for Arabidopsis *phyA* roots (**Figures 6A, B**). As in Arabidopsis, the tomato *pDR5::YFP* reporter line showed that the auxin response in the RAM was significantly reduced in the LGR condition compared to the DGR condition (**Figures 6C, D**). However, gene expression of the tomato orthologue of *AtYUC6*, *ToFZY2* (Expósito-Rodríguez et al., 2011), was similar in both conditions, indicating that this gene does not play a role in light-induced root growth inhibition (**Figure 6E**). For the *AtYUC4* orthologue, *ToFZY1* (Expósito-Rodríguez et al., 2011), a close to significant (p=0.08) decrease in expression was observed in LGR seedlings. To summarise, our data suggests that the PHY-triggered and auxin-modulated growth inhibition by light is conserved between Arabidopsis and tomato, but that not all components of the signalling pathway act in the same way or are shared between these two species.

Discussion

Culturing Arabidopsis seedlings on growth medium in petri dishes allows for an easy way to study root growth and development. However, the majority of these *in vitro* systems leave the roots exposed to light, making this system quite different from natural growth conditions in the soil. Although a number of studies have warned about negative effects of direct light on root growth and development (Yokawa et al., 2014; Moni et al., 2015), most studies still rely

on LGR systems for *in vitro* Arabidopsis research. To demonstrate the consequences of using LGR systems, we aimed to elucidate exactly how direct root illumination affects root growth. Whereas light perception in the shoot stimulates root growth and development, direct illumination of roots has been shown to reduce root growth. Furthermore, direct illumination of roots also influences lateral root emergence and distribution, anthocyanin accumulation and even flowering time (Sassi et al., 2012; Silva-Navas et al., 2015). Since the effects of root illumination are so diverse, they are more likely to be caused by photoreceptor signalling than by light-induced stresses such as ROS or DNA damage. So far, studies on root-localised photoreceptor signalling have been somewhat contradictive. Analysis of root growth in double cryptochrome and phototropin mutants, alongside blue LED treatments indicated that inhibition of root growth is likely to be mediated by blue light photoreceptors (Silva-Navas et al., 2015). In contrast, experiments with tissue-specific deficiency in PHY chromophores suggested that root PHYs, and not shoot PHYs, are required for inhibition of primary root elongation (Costigan et al., 2011). In this study, we identified PHYA and PHYB as regulators of root growth based on a screen of single photoreceptor mutants. For this reason, we cannot fully exclude some functional redundancy with blue light photoreceptors, as was indicated by Silva-Navas and colleagues (Silva-Navas et al., 2015). However, our experiments with coloured plastic indicated that R and FR, but not blue light, are reducing root growth. Additional grafting experiments confirmed that both root-localised PHYA and PHYB are required for light sensitivity, indicating that these photoreceptors are the main regulators of root growth inhibition in the LGR condition. When we considered downstream signalling components, PIFs seemed the most likely targets, since

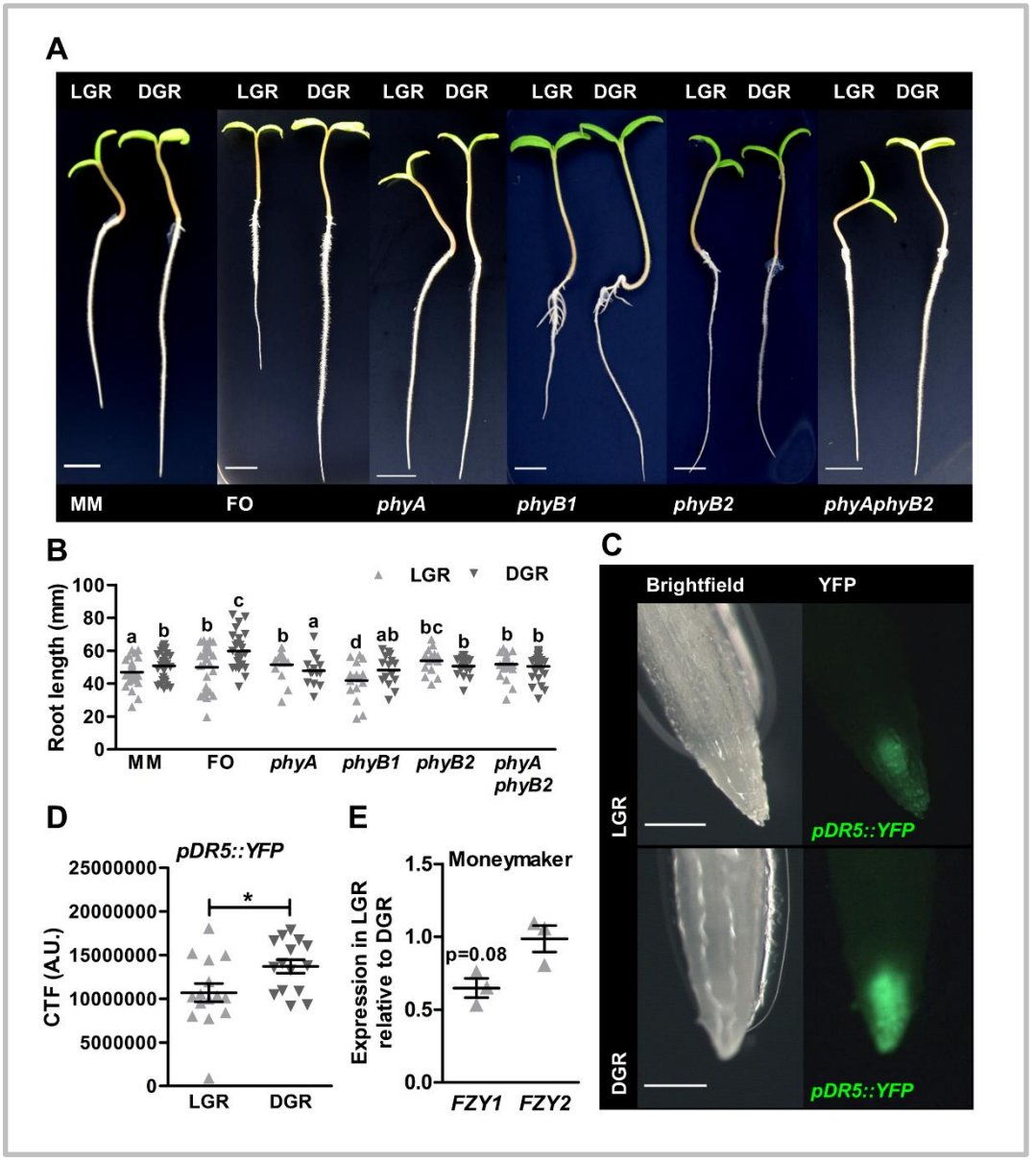

PIF signalling is exclusive for PHYA and PHYB. Although PIF3 has been shown to induce primary root growth inhibition in Arabidopsis (Bai et al., 2014), *pif3* mutants remained sensitive to the LGR condition, indicating that

Figure 6: Light-induced inhibition of root growth is (partially) conserved between Arabidopsis and tomato.
A. Representative 5-day-old tomato seedlings of wild-type cultivars Moneymaker (MM) and Foundation (FO), and of *phy* mutants (in MM background) grown in the LGR or the DGR condition. For presentation purposes, seedlings were transferred to black agarose plates before photographing. **B.** Quantification of the primary root length of 5-day-old MM, FO, and *phy* seedlings grown in the LGR or DGR condition. **C.** Stereo-fluorescence images of the root apical meristem (RAM) of *pDR5::YFP* tomato (M82) seedlings grown in the LGR or DGR condition. **D.** Quantification of the corrected total fluorescence (CTF) of *pDR5::YFP* in the RAM. **E.** Quantitative RT-PCR analysis of expression of *AtYUC4* orthologue *ToFZY1* and *AtYUC6* orthologue *ToFZY2* in the RAM of 5-day-old MM tomato seedlings grown in the LGR condition, relative to the DGR condition. Primary root lengths in **B** were compared using a one-way ANOVA followed by a Tukey's test. Letters **a**, **b**, **c**, and **d** indicate statistically different values, $p<0.05$. In **D**-**E**, the LGR condition was compared to the DGR condition using a two-sided Student's *t*-test (*$p<0.05$). Scale bars indicate 1 cm in **A**, and 0.5 mm in **C**. In **B** (n=30), **D** (n=20) and **E** (n=3), the horizontal line indicates the mean, error bars represent standard error of the mean (for some not visible due to limited variation) and triangles indicate values of biologically independent observations. Similar results were obtained from three (**A**-**B**, **E**), or from two independent experiments (**C**-**D**).

its function in primary root growth inhibition is initiated in the shoot and not in the root. Until now, no clear role has been described for PIF1 and PIF4 in regulation of root growth. Here we show for the first time that PIF1 and PIF4

have specific functions in regulation of root growth. Our analysis of the *pDR5::GFP* reporter and quantitative RT-PCR in *pif* mutants showed that, in the DGR condition, PIF1 and PIF4 stimulate local auxin biosynthesis in the RAM by elevating *YUC4* and *YUC6* expression. Since root cells are extremely sensitive to auxin, slight changes in local auxin concentrations can have great consequences (Thimann, 1937). Our analysis of the *pDR5::GFP* reporter in combination with NAA treatments revealed that endogenous auxin levels in dark-grown roots are close to optimal, whereas, in light-grown roots, they are greatly reduced, resulting in shorter roots. The close-to-optimal auxin levels in the DGR condition might explain previously reported increased sensitivity to indole-3-acetic acid (IAA) in DGR seedlings as well (Silva-Navas et al., 2015). With this experiment, we showed not only that inhibition of root growth by light is mediated by auxin, but we also demonstrated once more that the LGR *in vitro* system leads to suboptimal root growth. Based on our observations in Arabidopsis we propose a model where under natural circumstances, when roots are grown in darkness, PIF1 and PIF4 promote expression of *YUC6*, whereas PIF1 also promotes *YUC4* expression (**Figure 7**). This results in local auxin biosynthesis in the RAM, and thus in auxin levels that are close-to-optimal for root growth. When roots are exposed to light, however, such as in the widely used LGR *in vitro* system or in aeroponics, local PHYA and PHYB photoreceptors are activated. In light conditions with a low R/FR ratio, PHYA converts from the inactive PHYAfr conformation to the active PHYAr conformation that inhibits PIF1. Conversely, a high R/FR ratio converts the inactive PHYBr to the active PHYBfr that inhibits PIF4. Therefore, all light conditions that include either R or FR light, or both, will result in PIF inhibition, leading to a decrease in local auxin biosynthesis. As a result,

suboptimal auxin levels in the RAM lead to reduced primary root growth in LGR seedlings. However, light responses observed in the genetic model Arabidopsis do not always translate to an economically important crop such as tomato (**chapter 3**). By including tomato seedlings in this study, we could show that this mechanism is also present in a horticultural crop, albeit that the components of the signalling pathway are not completely conserved. This implies that the use of aeroponics or light-transmittable substrates could lead to suboptimal root growth in crops, which could result in decreased tolerance to a range of abiotic stresses (Koevoets et al., 2016). On the other

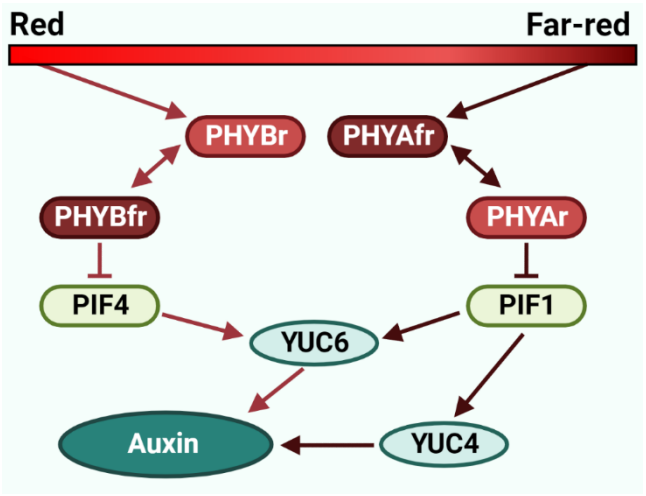

Figure 7: Model for root growth inhibition by local light perception in Arabidopsis roots.
Direct illumination of seedling roots with either red (R) or far-red (FR) light inhibits auxin biosynthesis which ultimately results in decreased primary root growth. In response to FR light, phytochrome A (PHYA) converts from the inactive PHYAfr state to the active PHYAr state and translocates to the nucleus where it inhibits PHYTOCHROME INTERACTING FACTOR 1 (PIF1). As a result, expression levels of *YUCCA 4* (*YUC4*) and *YUC6* are decreased. Similarly, in response to R light, PHYB converts from the inactive PHYBr state to the active PHYBfr state and inhibits PIF4 in the nucleus, thereby reducing *YUC6* expression. In both cases this leads to lower auxin levels in the RAM that are suboptimal for root growth.

hand, additional research into the root response to different spectral qualities might provide us with new ways to steer root architecture towards better crop performance. For example, light quality responses in the roots might be genetically linked to yield-associated traits in tomato (Alaguero-Cordovilla et al., 2018). Moreover, root illumination can influence flowering time in Arabidopsis (Silva-Navas et al., 2015), suggesting that light responses in the root might even influence shoot development and the timing of developmental phase transitions, thereby opening up new research possibilities towards crop improvement. Finally, the big question that remains to be answered is why plants have developed this molecular mechanism in response to root illumination. Since roots are actively stimulated to grow into the soil via gravitropism and negative phototropism (Harmer and Brooks, 2018), it is not entirely surprising that roots develop better in the darkness. But why would plants actively inhibit root growth when exposed to light? A possible reason might be that root inhibition by light somehow relates to negative phototropism. Previous studies have shown that light affects root halotropism and the gravitropic response, indicating its importance in tropic responses (Yokawa et al., 2011; Silva-Navas et al., 2015). Although negative phototropism is primarily regulated by the blue light receptor PHOT1, it has been suggested that PHYA interacts with PHOT1 during root phototropism, possibly by modulating its intracellular distribution, or through induction of PHYTOCHROME KINASE SUBSTRATE 1 (Boccalandro et al., 2008; Han et al., 2008). Moreover, a PHYA-mediated decrease of auxin in the RAM of light-grown roots might aid to establish the auxin gradient that is required for root bending during tropic responses. This, however, does not explain the PHYB response in the LGR condition. Aside from its role in light signalling,

PHYB is a known thermosensor that, together with PIF4, embodies the main signalling hub in regulation of temperature responses (Casal and Balasubramanian, 2019). Since exposure of roots to light likely rises the root temperature as well, the PHYB light response in roots could be correlated to temperature responses. Substantial increases in root temperature result in decreased nutrient uptake, enhanced respiration, and overall growth inhibition (Du and Tachibana, 1994). A light-induced decrease in RAM size could contribute to, or be a result of, root cell respiration induced by high temperature. In addition, PHYB-PIF4 signalling regulates auxin biosynthesis in hypocotyls in response to heat stress (Sun et al., 2012), suggesting the possibility that, in roots, light and temperature coregulate auxin levels via PHYB-PIF4 to avoid water and nutrient loss.

Materials and Methods

Growth conditions and light treatments.

In all experiments, seedlings were grown at a 16h photoperiod, under white TL lights with a measured photon flux density of 150±10 μmol m^{-2} s^{-1}, a temperature of 21°C and 50% relative humidity. Two different light treatments were included: (1) seedlings were grown completely exposed to light (light-grown roots or LGR); or (2) seedlings were grown in a more "natural" light environment with shoots exposed to light and roots shielded from light using black paper covers: (dark-grown roots or DGR) (**Figure S1**) (based on Silva-Navas et al., 2015).

Plant lines and seed germination.

Wild-type seedlings of *Arabidopsis thaliana* (Arabidopsis) and *Solanum lycopersicum* (tomato) were used as controls in this study. For Arabidopsis two ecotypes were included: Columbia (Col-0) and Landsberg *erecta* (L*er*). For tomato, the Moneymaker (MM) cultivar and the commercial hybrid line Foundation (FO) were used. All Arabidopsis and tomato mutants and reporter lines that were used are listed in **Table S2**. Arabidopsis single mutants *phyA*, *phyB*, *pif1*, and *pif4* (all in Col-0 background) have been described before (Mayfield et al., 2007; Ruckle et al., 2007; Leivar et al., 2008a; Stephenson et al., 2009), and were crossed with *pDR5::GFP* to monitor auxin responses in these lines. Prior to the experiments all mutant lines and crosses were genotyped using the primers listed in **Table S3** and if required CAPS / PCR-RFLP markers described in **Table S4** (Nam et al., 1989; Konieczny and Ausubel, 1993). Arabidopsis and tomato seeds were surface sterilised by incubating for 1 minute in 70% ethanol and 10 minutes in a 2-fold diluted commercial bleach solution (1% chlorine). Subsequently the seeds were washed five times with sterile water. Arabidopsis seeds were stratified for 5 days at 4°C in darkness and germinated on square plates (#688102, Greiner Bio-One^{TM}) containing MA medium (Masson and Paszkowski, 1992) supplemented with 1% (w/v) sucrose and 0.8% (w/v) Daishin agar. Arabidopsis seeds were germinated by placing the plates vertically in the two light conditions described above. Sterile tomato seeds were placed on sterilised, wet filter paper (#1001325, Whatman®) using forceps and were germinated in darkness at 21°C for 5 days. Germinated seeds were moved from

the filters to square plates containing solid MA medium and placed vertically in the two light conditions described above.

In vitro analysis of seedling growth.

At 7 days after germination (DAG), Arabidopsis seedlings were photographed, and primary root length and hypocotyl length were measured. The shoot-root ratio was calculated based on these measurements. Tomato seedlings were photographed at 5 DAG for primary root length measurements. To monitor the response of Arabidopsis seedlings to exogenous auxin, 4-day-old seedlings were transferred to square plates containing MA medium supplemented with 0, 5, 10, 20, 30, 40 or 50 nM 1-naphthaleneacetic acid (NAA). The increase in primary root length between 0 and 6 days after NAA treatment was measured. At 6 days after NAA treatment, *pDR5::GFP* seedlings were analysed under the confocal microscope. To analyse root-localised versus shoot-localised phytochrome functions, 4-day-old Arabidopsis seedlings grown in the LGR condition were grafted as described previously (Marsch-Martínez et al., 2013) in the following combinations: wild type/wild type (positive control); mutant/mutant (negative control); wild type/mutant (mutation only present in roots) and mutant/wild type (mutation only present in shoots). At 5 days after grafting, successful grafts were photographed to measure the post-grafting increase in primary root growth and analysed under the confocal microscope. To analyse the response of roots to light quality, the roots were covered with red translucent plastic (RGR) or blue translucent plastic (BGR). To avoid any additional effects of decreased light intensity, LGR seedlings were wrapped with white translucent plastic in this experiment. The primary root length was

measured after 7 days of growth under coloured plastic. All measurements were performed with ImageJ (Fiji) (Schindelin et al., 2012).

Microscopy analysis.

For confocal images of Arabidopsis roots, 7-day-old seedlings were stained with 10 µg/ml propidium iodide (PI) for 5 minutes and then mounted onto a glass slide in water with a cover slip. To visualise *pDR5::GFP* and PI staining in root tips, a Zeiss LSM5 Exciter/AxioImager equipped with a 40x oil objective and respectively a 488 nm argon laser and a 505-530 nm band pass filter or 600 nm long pass filter was used. For images of tomato roots, 5-day-old seedlings were mounted on a glass slide and imaged with a Leica MZ16FA equipped with a Leica DFC420C camera. YFP fluorescence was detected using a 510/20 nm excitation filter and a 560/40 nm emission filter. To quantify the fluorescent signals, the corrected total cell fluorescence method (McCloy et al., 2014) was slightly adjusted to quantify the corrected total fluorescence (CTF) of the root apex. CTF = integrated density (sum of all pixel intensities) – (area of root apex * mean fluorescence of background readings). All CTF measurements were performed in ImageJ (Fiji) and are expressed in Arbitrary Units (A.U.).

RNA extraction and qRT-PCR.

Root tips of 7-day-old Arabidopsis seedlings or 5-day-old tomato seedlings were pooled (±80 per RNA sample), frozen in liquid nitrogen, and ground with a TissueLyser II (#85300, Qiagen). Total RNA was extracted from the ground tissue using a RNeasy© Plant Mini kit (#74904, Qiagen), and used for first strand cDNA synthesis with the RevertAid First Strand cDNA Synthesis kit

(#K1621, Thermo Scientific™). For qRT-PCR, the cDNA was diluted 10x and used with TB Green Premix Ex Taq II (Tli RNase H Plus) (#RR820B, Takara) and the CFX96 TouchTM Real-Time PCR Detection System (#1855196, Bio-Rad). CT values were obtained using Bio-Rad CFX manager 3.1. Normalisation was done according to the ΔΔCt method with *PP2A* (At2g42500) and *TIP41* (Solyc10g049850) as reference genes for Arabidopsis and tomato, respectively (Pfaffl, 2001). All primers that were used for qRT-PCR are listed in **Table S3.**

Linear regression analysis.

The correlation coefficient (*r*) was calculated using the equation below, where *x* represents the NAA concentration, and *y* represents the *pDR5::GFP* signal.

$$r = \frac{\sum(x_i - \bar{x})(y_i - \bar{y})}{\sqrt{\sum(x_i - \bar{x})^2 \sum(y_i - \bar{y})^2}}$$

To calculate the linear regression coefficients *a* (y-intercept) and *b* (slope), the following equations were used, where $\sigma(x,y)$ represents the covariance of *x* and *y*, and $\sigma(x)$ represents the variance of *x*.

$$a = \bar{y} - b\bar{x} \qquad\qquad b = \frac{\sigma(x,y)}{\sigma(x)}$$

Statistical analysis and figures.

All phenotyping and microscopy experiments were performed with 20 or 30 biologically independent seedlings for tomato or Arabidopsis, respectively. In experiments that included only wild-type seedlings, the LGR condition was compared to the DGR condition using a two-sided Student's *t*-test. Experiments that included NAA treatments, or wild type versus mutant comparisons were statistically analysed using a one-way ANOVA followed by a Tukey's honestly significant different (HSD) post hoc test. In qRT-PCR experiments, three biological replicates (RNA isolated from ± 80 root tips) were included, with three technical replicates each. For each plant line, normalised levels of gene expression in the LGR condition were compared to the DGR condition using a two-sided Student's *t*-test. For the linear regression analysis, regression coefficient *b* of the LGR condition was compared to regression coefficient *b* of the DGR condition as previously described (Andrade and Estévez-Pérez, 2014). All measurements were plotted into graphs using GraphPad Prism 5 software. All photographs were taken with a Nikon D5300 camera and edited in ImageJ (Fiji). Schematic models were generated with BioRender software. Final figures were assembled using Microsoft PowerPoint.

Author Contributions

KS and RO conceived and designed the experiments. KS performed the experiments and the statistical analysis. KS and RO analysed the results and wrote the manuscript. Both authors contributed to manuscript revision.

Funding

This work was part of the research programme “LED it be 50%” with project number 14212, which is partly financed by the Dutch Research Council (NWO).

Acknowledgements

We would like to thank Nunhems Netherlands BV for providing seeds of their commercial tomato hybrid line Foundation, and Cris Kuhlemeier for providing seeds of the tomato M82 *pDR5::YFP* reporter line. We thank Dália Alves Carvalho for help with propagation and genotyping of tomato mutants. Furthermore we acknowledge Thomas van der Toorn and Daan Kloosterman for help in optimizing the DGR system, Gerda Lamers for assistance with microscopy, Yohanna Miotto for help in optimizing grafting protocols, and Nick Surtel for assistance with the “coloured plastic” experiments.

References

Aceves-García, P., Álvarez-Buylla, E. R., Garay-Arroyo, A., García-Ponce, B., Muñoz, R., and Sánchez, M. de la P. (2016). Root architecture diversity and meristem dynamics in different populations of *Arabidopsis thaliana*. *Front. Plant Sci.* 7, 1–14.

Alaguero-Cordovilla, A., Gran-Gómez, F. J., Tormos-Moltó, S., and Pérez-Pérez, J. M. (2018). Morphological characterization of root system architecture in diverse tomato genotypes during early growth. *Int. J. Mol. Sci.* 19, 3888.

Andrade, J. M., and Estévez-Pérez, M. G. (2014). Statistical comparison of the slopes of two regression lines: A tutorial. *Anal. Chim. Acta* 838, 1–12.

Arsovski, A. A., Galstyan, A., Guseman, J. M., and Nemhauser, J. L. (2012). Photomorphogenesis. *Arab. B.* 10, e0147.

Bai, S., Yao, T., Li, M., Guo, X., Zhang, Y., Zhu, S., and He, Y. (2014). PIF3 is involved in the primary root growth inhibition of *Arabidopsis* induced by nitric oxide in the light. *Mol. Plant* 7, 616–625.

Bainbridge, K., Guyomarc'h S., Bayer, E., Swarup, R., Bennet, M., Mandel, T., and Kuhlemeier, C. (2008). Auxin influx carriers stabilize phyllotactic patterning. *Genes Dev.* 22, 810-823.

Baskin, T. I. (2013). Patterns of root growth acclimation: Constant processes, changing boundaries. *Wiley Interdiscip. Rev. Dev. Biol.* 2, 65–73.

Ben-Gera, H., Shwartz, I., Shao, M. R., Shani, E., Estelle, M., and Ori, N. (2012). ENTIRE and
GOBLET promote leaflet development in tomato by modulating auxin response. *Plant J.* 70, 903-915.

Boccalandro, H. E., De Simone, S. N., Bergmann-Honsberger, A., Schepens, I., Fankhauser, C., and Casal, J. J. (2008). Phytochrome kinase substrate1 regulates root phototropism and gravitropism. *Plant Physiol.* 146, 108–115.

Casal, J. J., and Balasubramanian, S. (2019). Thermomorphogenesis. *Annu. Rev. Plant Biol.* 70**,** 321-346.

Chen, X., Yao, Q., Gao, X., Jiang, C., Harberd, N. P., and Fu, X. (2016). Shoot-to-root mobile transcription factor HY5 coordinates plant carbon and nitrogen acquisition. *Curr. Biol.* 26, 640–646.

Cheng, Y., Dai, X., and Zhao, Y. (2006)**.** Auxin biosynthesis by the YUCCA flavin monooxygenases controls the formation of floral organs and vascular tissues in Arabidopsis. *Genes Dev.* 20), 1790-1799.

Christians, M. J., Gingerich, D. J., Hua, Z., Lauer, T. D., and Vierstra, R. D. (2012). The light-response BTB1 and BTB2 proteins assemble nuclear ubiquitin ligases that modify phytochrome B and D signaling in Arabidopsis. *Plant Physiol.* 160, 118-134.

Costigan, S. E., Warnasooriya, S. N., Humphries, B. A., and Montgomery, B. L. (2011). Root-localized phytochrome chromophore synthesis is required for photoregulation of root elongation and impacts root sensitivity to jasmonic acid in Arabidopsis. *Plant Physiol.* 157, 1138–1150.

de Wit, M., Galvão, V. C., and Fankhauser, C. (2016). Light-mediated hormonal regulation of plant growth and development. *Annu. Rev. Plant Biol.* 67, 513–537.

Du, Y. C., and Tachibana, S. (1994). Effect of supraoptimal root temperature on the growth, root respiration and sugar content of cucumber plants. *Sci. Hortic.* 58, 289–301.

Expósito-Rodríguez, M., Borges, A. A., Borges-Pérez, A., and Pérez, J. A. (2011). Gene structure and spatiotemporal expression profile of tomato genes encoding YUCCA-like flavin monooxygenases: The ToFZY gene family. *Plant Physiol. Biochem.* 49, 782–791.

Franklin, K. A., Lee, S. H., Patel, D., Kumar, S. V., Spartz, A. K., Gu, C., Ye, S., Yu, P., Breen, G., Cohen, J. D., Wigge, P. A., and Gray, W.M. (2011). Phytochrome-Interacting Factor 4 (PIF4) regulates auxin biosynthesis at high temperature. *Proc. Natl. Acad. Sci. U. S. A.* 108, 20231–20235.

Guenot, B., Bayer, E., Kierzkowski, D., Smith, R. S., Mandel, T., Zádniková, P., Benková, E.,

and Kuhlemeier, C. (2012). PIN1-independent leaf initiation in Arabidopsis. *Plant Physiol.* 159, 1501-1510.

Guo, H., Yang, H., Mockler, T. C., and Lin, C. (1998). Regulation of flowering time by
Arabidopsis photoreceptors. *Science* 279, 1360-1363.

Han, I. S., Tseng, T. S., Eisinger, W., and Briggs, W. R. (2008). Phytochrome A regulates the intracellular distribution of phototropin 1-green fluorescent protein in *Arabidopsis thaliana*. *Plant Cell* 20, 2835–2847.

Harmer, S. L., and Brooks, C. J. (2018). Growth-mediated plant movements: hidden in plain sight. *Curr. Opin. Plant Biol.* 41, 89–94.

Kim, J., Yi, H., Choi, G., Shin, B., Song, P. S., and Choi, G. (2003). Functional characterization of
phytochrome interacting factor 3 in phytochrome-mediated light signal transduction. *Plant Cell* 15, 2399-2407.

Koevoets, I. T., Venema, J. H., Elzenga, J. T. M., and Testerink, C. (2016). Roots withstanding their environment: Exploiting root system architecture responses to abiotic stress to improve crop tolerance. *Front. Plant Sci.* 7, 1–19.

Konieczny, A., and Ausubel, F. M. (1993). A procedure for mapping Arabidopsis mutations using co-dominant ecotype-specific PCR-based markers. *Plant J.* 4, 403–410.

Lee, H. J., Ha, J. H., Kim, S. G., Choi, H. K., Kim, Z. H., Han, Y. J., Kim, J. Il, Oh, Y., Fragoso, V., Shin, K., Hyeon, T., Choi, H. G., Oh, K. H., Baldwin, I. T., and Park, C. M. (2016). Stem-piped light activates phytochrome B to trigger light responses in *Arabidopsis thaliana* roots. *Sci. Signal.* 9, 1–10.

Lee, H. J., Park, Y. J., Ha, J. H., Baldwin, I. T., and Park, C. M. (2017). Multiple routes of light signaling during root photomorphogenesis. *Trends Plant Sci.* 22, 803–812.

Leivar, P., Monte, E., Al-Sady, B., Carle, C., Storer, A., Alonso, J. M., Ecker, J. R., and Quail, P. H. (2008a). The Arabidopsis phytochrome-interacting factor

PIF7, together with PIF3 and PIF4, regulates responses to prolonged red light by modulating phyB levels. *Plant Cell* 20, 337–352.

Leivar, P., Monte, E., Oka, Y., Liu, T., Carle, C., Castillon, A., Huq, E., and Quail, P. H. (2008b). Multiple phytochrome-interacting bHLH transcription factors repress premature seedling photomorphogenesis in darkness. *Curr. Biol.* 18, 1815-1823.

Lejay, L., Wirth, J., Pervent, M., Cross, J. M. F., Tillard, P., and Gojon, A. (2008). Oxidative pentose phosphate pathway-dependent sugar sensing as a mechanism for regulation of root ion transporters by photosynthesis. *Plant Physiol.* 146, 2036–2053.

Marsch-Martínez, N., Franken, J., Gonzalez-Aguilera, K. L., de Folter, S., Angenent, G., and Alvarez-Buylla, E. R. (2013). An efficient flat-surface collar-free grafting method for *Arabidopsis thaliana* seedlings. *Plant Methods* 9, 1–9.

Masson, J., and Paszkowski, J. (1992). The culture response of *Arabidopsis thaliana* protoplasts is determined by the growth conditions of donor plants. *Plant J.* 2, 829–833.

Mayfield, J. D., Folta, K. M., Paul, A. L., and Ferl, R. J. (2007). The 14-3-3 proteins μ and υ influence transition to flowering and early phytochrome response. *Plant Physiol.* 145, 1692–1702.

McCloy, R. A., Rogers, S., Caldon, C. E., Lorca, T., Castro, A., and Burgess, A. (2014). Partial inhibition of Cdk1 in G2 phase overrides the SAC and decouples mitotic events. *Cell Cycle* 13, 1400–1412.

McElver, J., Tzafrir, I., Aux, G., Rogers, R., Ashby, C., Smith, K., Thomas, C., Schetter, A., Zhou, Q., Cushman, M. A., Tossberg, J., Nickle, T., Levin, J. Z., Law, M., Meinke, D., and Patton, D. (2001). Insertional mutagenesis of genes required for seed development in *Arabidopsis thaliana*. *Genetics* 159, 1751-1763.

Moni, A., Lee, A. Y., Briggs, W. R., and Han, I. S. (2015). The blue light receptor Phototropin 1 suppresses lateral root growth by controlling cell elongation. *Plant Biol.* 17, 34–40.

Monte, E., Alonso, J. M., Ecker, J. R., Zhang, Y., Li, X., Young, J., Austin-Phillips, S., and Quail, P. H. (2003). Isolation and characterization of phyC mutants in Arabidopsis reveals complex crosstalk between phytochrome signaling pathways. *Plant Cell* 15, 1962-1980.

Nam, H. G., Giraudat, J., Den Boer, B., Moonan, F., Loos, W., Hauge, B. M., and Goodman, H. M. (1989). Restriction fragment length polymorphism linkage map of *Arabidopsis thaliana*. *Plant Cell* 1, 699–705.

Ottenschlager, I., Wolff, P., Wolverton, C., Bhalerao, R. P., Sandberg, G., Ishikawa, H., Evans, M., and Palme, K. (2003). Gravity-regulated differential auxin transport from columella to lateral root cap cells. *Proc. Natl. Acad. Sci. U. S. A.* 100, 2987-2991.

Petricka, J. J., Winter, C. M., and Benfey, P. N. (2012). Control of Arabidopsis root development. *Annu. Rev. Plant Biol.* 63, 563–590.

Pfaffl, M. W. (2001). A new mathematical model for relative quantification in real-time RT-PCR. *Nucleic Acids Res.* 29, e45.

Pham, V. N., Kathare, P. K., and Huq, E. (2018). Phytochromes and phytochrome interacting factors. *Plant Physiol.* 176, 1025–1038.

Podolec, R., and Ulm, R. (2018). Photoreceptor-mediated regulation of the COP1/SPA E3 ubiquitin ligase. *Curr. Opin. Plant Biol.* 45, 18–25.

Redei, G. P. (1992), A heuristic glance at the past of Arabidopsis genetics. *Methods in Arabidopsis Research*, 1-15.

Reed, J. W., Nagatani, A., Elich, T. D., Fagan, M., and Chory, J. (1994). Phytochrome A and phytochrome B have overlapping but distinct functions in Arabidopsis development. *Plant Physiol.* 104, 1139-1149.

Ruckle, M. E., DeMarco, S. M., and Larkin, R. M. (2007). Plastid signals remodel light signaling networks and are essential for efficient chloroplast biogenesis in Arabidopsis. *Plant Cell* 19, 3944–3960.

Sassi, M., Lu, Y., Zhang, Y., Wang, J., Dhonukshe, P., Blilou, I., Dai, M., Li, J., Gong, X., Jaillais, Y., Yu, X., Traas, J., Ruberti, I., Wang, H., Scheres, B., Vernoux, T., and Xu, J. (2012). COP1 mediates the coordination of root and

shoot growth by light through modulation of PIN1- and PIN2-dependent auxin transport in Arabidopsis. *Dev.* 139, 3402–3412.

Schindelin, J., Arganda-Carreras, I., Frise, E., Kaynig, V., Longair, M., Pietzsch, T., Preibisch, S., Rueden, C., Saalfeld, S., Schmid, B., Tinevez, J. Y., White, D. J., Hartenstein, V., Eliceiri, K., Tomancak, P., and Cardona, A. (2012). Fiji: An open-source platform for biological-image analysis. *Nat. Methods* 9, 676–682.

Silva-Navas, J., Moreno-Risueno, M. A., Manzano, C., Pallero-Baena, M., Navarro-Neila, S., Téllez-Robledo, B., Garcia-Mina, J. M., Baigorri, R., Gallego, F. J., and Del Pozo, J. C. (2015). D-Root: A system for cultivating plants with the roots in darkness or under different light conditions. *Plant J.* 84, 244–255.

Smith, R. S., Guyomarc'h, S., Mandel, T., Reinhardt, D., Kuhlemeier, C., and Prusinkiewicz, P. (2006). A plausible model of phyllotaxis. *Proc. Natl. Acad. Sci. U. S. A.* 103, 1301-1306.

Stephenson, P. G., Fankhauser, C., and Terry, M. J. (2009). PIF3 is a repressor of chloroplast development. *Proc. Natl. Acad. Sci. U. S. A.* 106, 7654–7659.

Sun, J., Qi, L., Li, Y., Chu, J., and Li, C. (2012). Pif4-mediated activation of yucca8 expression integrates temperature into the auxin pathway in regulating Arabidopsis hypocotyl growth. *PLoS Genet.* 8, e1002594.

Thimann, K. V. (1937). On the nature of inhibitions caused by auxin. *Am. J. Bot.* 24, 407.

Van Gelderen, K., Kang, C., and Pierik, R. (2018). Light signaling, root development, and plasticity. *Plant Physiol.* 176, 1049–1060.

Van Tuinen, A., Kerckhoffs, L. H. J., Nagatani, A., Kendrick, R. E., and Koornneef, M. (1995a). Far-red light-insensitive, phytochrome A-deficient mutants of tomato. *Mol. Gen. Genet.* 246, 133-141.

Van Tuinen, A., Kerckhoffs, L. H. J., Nagatani, A., Kendrick, R. E., and Koornneef, M. (1995b). A temporarily red light-insensitive mutant of tomato lacks a light-stable, B-like phytochrome. *Plant Physiol.* 108, 939-947.

Warnasooriya, S. N., Porter, K. J., and Montgomery, B. L. (2011). Tissue- and isoform-specific phytochrome regulation of light-dependent anthocyanin accumulation in *Arabidopsis thaliana. Plant Signal. Behav.* 6, 624-631.

Weller, J. L., Schreuder, M. E. L., Smith, H., Koornneef, M., and Kendrick, R. E. (2000). Physiological interactions of phytochromes A, B1 and B2 in the control of development in tomato. *Plant J.* 24, 345-356.

Yokawa, K., Kagenishi, T., Kawano, T., Mancuso, S., and Baluška, F. (2011). Illumination of Arabidopsis roots induces immediate burst of ROS production. *Plant Signal. Behav.* 6, 1460–1464.

Yokawa, K., Fasano, R., Kagenishi, T., and Baluška, F. (2014). Light as stress factor to plant roots – Case of root halotropism. *Front. Plant Sci.* 5, 1–9.

Supplementary Material (Tables S1-S4 and Figures S1-S3)

Table S1: Linear regression analysis.

Linear regression analysis of the correlation between NAA concentration and *pDR5::GFP* expression in the RAM. *y*-values are the mean values of the dot plot shown in Figure 2D. $\sigma(x,y)$ = covariance of *x*- and *y*-values, $\sigma(x)$ = variance of *x*-values, and $\sigma(y)$ = variance of *y*-values. Regression coefficient *a* indicates the y-intercept, and regression coefficient *b* indicates the slope.

Light condition	**NAA concentration (*x*)**	**GFP signal (*y*)**	$x_i - x_{mean}$	$y_i - y_{mean}$	$\sigma(x,y)$	$\sigma(x)$	$\sigma(y)$
LGR	0	277979	-25	-151755	3793879	625	23029630610
	10	333101	-15	-96633	1449497	225	9337968900
	20	414728	-5	-15006	75031	25	225185038
	30	454278	5	24544	122719	25	602399755
	40	534336	15	104601	1569027	225	10941543537
	50	563983	25	134249	3356221	625	18022749251
Mean	**25**	**429734**	**0**	**0**	**1727729**	**292**	**10359912848**
DGR	0	525449	-8.75	-64573	565011	76.6	4169640043
	5	565031	-3.75	-24991	93715	14.1	624537586
	10	614962	1.25	24940	31175	1.6	622016070
	20	654645	11.25	64623	727012	126.6	4176164441
Mean	**8.75**	**590022**	**0**	**0**	**354228**	**54.7**	**2398089535**
	Correlation coefficient (*r*)	**Regression coefficient (*a*)**			**Regression coefficient (*b*)**		
LGR	0.993	281643			5924		
DGR	0.978	533345			6477		
	p-value slope comparison (*b*)						
LGR vs DGR	0.609						

Table S2: Plant lines used in this study.

Arabidopsis mutant lines were obtained from Nottingham Arabidopsis Stock Centre (NASC). Tomato mutant lines were obtained from Tomato Genetics Resource Centre (TGRC).

Plant line	Description	Source	Reference
Arabidopsis			
Columbia (Col-0)	Natural Arabidopsis accession	-	Redei, 1992
Landsberg *erecta* (L*er*)	Natural Arabidopsis accession	-	Redei, 1992
Moneymaker (MM)	Standard non-hybrid cultivar	Nunhems	-
Foundation (FO)	Commercial hybrid	Nunhems	-
yuc4 (SM_3_16128)	Transposon insertion in exon of At5g11320	-	Cheng et al., 2006
yuc6 (SALK_093708)	T-DNA insertion in intron of At5g25620	-	Cheng et al., 2006
phyA (SALK_014575)	T-DNA insertion in exon of At1g09570	NASC	Ruckle et al., 2007
phyB (SALK_ 022035)	T-DNA insertion in exon of At2g18790	NASC	Mayfield et al., 2007
phyC (phyC-3)	3 kbp deletion in At5g35840	NASC	Monte et al., 2003
phyD (SALK_027956)	T-DNA insertion in exon of At4g16250	NASC	Christians et al., 2012
phyE (SALK_092529)	T-DNA insertion in exon of At4g18130	NASC	Warnasooriya et al., 2011
cry1 (SALK_069292)	T-DNA insertion in exon of At4g08920	NASC	Ruckle et al., 2007
cry2 (cry2-1)	Large deletion (2/3) in At1g04400	NASC	Guo et al., 1998
phot1 (SAIL_1232_C01)	T-DNA insertion in exon of At3g45780	NASC	McElver et al., 2001
phot2 (SALK_142275)	T-DNA insertion in exon of At5g58140	NASC	Ruckle et al., 2007
phyAphyB (phyA-201 phyB-5)	Substitution Q980STOP in At1g09570 x substitution W552STOP in At2g18790	NASC	Reed et al., 1994
pif1 (SAIL_256_G07)	T-DNA insertion in exon of At2g20180	NASC	Stephenson et al., 2009
pif3 (SALK_030753)	T-DNA insertion in intron of At1g09530	NASC	Kim et al., 2003
pif4 (SAIL_1288_E07)	T-DNA insertion in intron of At2g43010	NASC	Leivar et al., 2008a
pif1pif3pif4 (SAIL_256_G01, pif3-3, SAIL_1288_E07)	2.5 kbp deletion in At1g09530 x T-DNA insertion in At2g20180 and At2g43010	NASC	Leivar et al., 2008b
pin1 (SALK_047613)	T-DNA insertion in exon of At1g73590	NASC	Smith et al., 2006
pin2 (*eir1-1*)	Diepoxybutane mutation in exon of At5g57090	NASC	Guenot et al., 2012
pin4-3	Transposon insertion in exon of At2g01420	NASC	Guenot et al., 2012
pin7-2	T-DNA insertion in exon of At1g23080	NASC	Guenot et al., 2012
auxlaxq (*aux1-21, lax1, lax2, lax3)*	EMS mutation in exon of At2g38120 x T-DNA insertion in exon of At5g01240 x T-DNA insertion in exon of At2g21050 x T-DNA insertion in exon of At1g77690	NASC	Bainbridge et al., 2008
pDR5::GFP	Synthetic auxin-responsive reporter (Col-0)	-	Ottenschlager et al., 2003
phyA x pDR5::GFP	SALK_014575 crossed with DR5 reporter	-	This study
phyB x pDR5::GFP	SALK_022035 crossed with DR5 reporter	-	This study
pif1 x pDR5::GFP	SAIL_256_G07 crossed with DR5 reporter	-	This study
pif4 x pDR5::GFP	SAIL_1288_E07 crossed with DR5 reporter	-	This study
Tomato			
phyA (phyA-1)	Null-mutant (fri^1)	TGRC	Van Tuinen et al., 1995a
phyB1 (phyB1-1)	Null-mutant (tri^1)	TGRC	Van Tuinen et al., 1995b
phyB2 (phyB2-1)	Null-mutant (70F)	TGRC	Weller et al., 2000
phyAphyB2	Null-mutant (fri^1) x Null mutant (70F)	TGRC	Weller et al., 2000
pDR5::YFP	Synthetic auxin-responsive reporter (M82)	Kuhlemeier	Ben-Gera et al., 2012

Table S3: Primers used in this study.

Primer name	Target gene	Sequence 5'→3'	Experiment
LB1 (SAIL T-DNA)	N/A	GCCTTTTCAGAAATGGATAAATA	Genotyping
LBb1.3 (SALK T-DNA)	N/A	ATTTTGCCGATTTCGGAAC	Genotyping
Border seq (SM transposon)	N/A	TACGAATAAGAGCGTCCATTTTAGAGTGA	Genotyping
SALK_014575 (*phyA*) FW	At1g09570	CCAGTCAGCTCAGCAATTTTC	Genotyping
SALK_014575 (*phyA*) RV	At1g09570	AATGCAAAACATGCTAGGGTG	Genotyping
SALK_ 022035 (*phyB*) FW	At2g18790	CATCATCAGCATCATGTCACC	Genotyping
SALK_ 022035 (*phyB*) RV	At2g18790	TTCACGAAGGCAAAAGAGTTG	Genotyping
SM_3_16128 (*yuc4*) FW	At5g11320	CCCTTCTTAGACCTACTCTAC	Genotyping
SM_3_16128 (*yuc4*) RV	At5g11320	GCCCAACGTAGAATTAGCAAG	Genotyping
SALK_093708 (*yuc6*) FW	At5g25620	CCAGCCTTTGTATTTTCCCGT	Genotyping
SALK_093708 (*yuc6*) RV	At5g25620	CCGGAAAAAGGGTTCTTGTCG	Genotyping
phyA-201 (double mutant) FW	At1g09570	GAAGTGTTGACTGCTTCCACGAGT	Genotyping
phyA-201 (double mutant) RV	At1g09570	TAGCAAGATGCACAGAACGCC	Genotyping
phyB-5 (double mutant) FW	At2g18790	CGTGACGCGCCTGCTGGAATTGTT	Genotyping
phyB-5 (double mutant) RV	At2g18790	TCCATTGATGCAGCCTCCGGCA	Genotyping
phyC-3 FW	At5g35840	ATGTCATCGAACACTTCACG	Genotyping
phyC-3 RV	At5g35840	TCAAATCAAGGGAAATTCTG	Genotyping
SALK_027956 (*phyD*) FW	At4g16250	AACCCGGTAGAATCAGAATGG	Genotyping
SALK_027956 (*phyD*) RV	At4g16250	ATCGGTTACAGTGAAAATGCG	Genotyping
SALK_092529 (*phyE*) FW	At4g18130	AAAGAGGCGGTCTAGTTCAGC	Genotyping
SALK_092529 (*phyE*) RV	At4g18130	TATCAGTGGTTAAACCCGTCG	Genotyping
SALK_069292 (*cry1*) FW	At4g08920	TTCATGCCACTTGGTTAGACC	Genotyping
SALK_069292 (*cry1*) RV	At4g08920	TCCCGACAGACTGGATACATC	Genotyping
cry2-1 FW	At1g04400	ATGAAGATGGACAAAAAGAC	Genotyping
cry2-1 RV	At1g04400	TCATTTGCAACCATTTTTTC	Genotyping
SAIL_1232_C01 (*phot1*) FW	At3g45780	ACATAGGATGCAGCAGAAACG	Genotyping
SAIL_1232_C01 (*phot1*) RV	At3g45780	CAGTAGACTGGTGGGCTCTTG	Genotyping
SALK_142275 (*phot2*) FW	At5g58140	TCCATCTCCTTTGAATGATGC	Genotyping
SALK_142275 (*phot2*) RV	At5g58140	AGTGTCATTGCTCACGGATTC	Genotyping
phyA-1 FW	Solyc10g044670	TAACTGAATACACCATTCCCTTAACC	Genotyping
phyA-1 RV	Solyc10g044670	ATAATCGCTCTATAGTCACC	Genotyping
phyB1-1 FW	Solyc01g059870	CTAAAATTCAAAGAGGAGGTCAGATT	Genotyping
phyB1-1 RV	Solyc01g059870	GAAGGGGTAAAAAGGGTCCTAA	Genotyping
phyB2-1 FW	Solyc05g053410	GACGAGTAACATTCACATGA	Genotyping
phyB2-1 RV	Solyc05g053410	GCTTAGGCAACACTAGGTTA	Genotyping
SAIL_256_G07 (*pif1*) FW	At2g20180	AAGGAAGGAGGAGGAATAGGC	Genotyping
SAIL_256_G07 (*pif1*) RV	At2g20180	CATGAATTTCTCGAGGCTGAG	Genotyping
SALK_030753 (*pif3*) FW	At1g09530	AGTCTGTTGCTTCTGCTACGC	Genotyping
SALK_030753 (*pif3*) RV	At1g09530	TTGCATAAGGCATTCCCATAC	Genotyping
SAIL_1288_E07 (*pif4*) FW	At2g43010	AATACATTTTGCAGGCAATCG	Genotyping
SAIL_1288_E07 (*pif4*) RV	At2g43010	CGTAATGAAGTTGCACGTTTACTC	Genotyping
pif3-3 WT (triple mutant) FW	At1g09530	AGAAGCAATTTGGTCACCATGCTC	Genotyping
pif3-3 WT (triple mutant) RV	At1g09530	TGCATACAAATAGTCGATCGTATG	Genotyping
pif3-3 DEL (triple mutant) FW	At1g09530	GGTGTGTATGTGAGAAGGTACATCCATCG	Genotyping
pif3-3 DEL (triple mutant) RV	At1g09530	AAGCTTAGCTTTGGTGAGCCTGAAAAGCT	Genotyping
SALK_047613 (*pin1*) FW	At1g73590	TTCCATAAAGTCATGATTAAGCACA	Genotyping
SALK_047613 (*pin1*) RV	At1g73590	CGGTGGGAACAACATAAGCAA	Genotyping
eir1-1 (*pin2*) FW	At5g57090	GGTACCAAATGATCACCGGCAAAGACAT	Genotyping
eir1-1 (*pin2*) RV	At5g57090	GAAGAGATCATTGATGAGGC	Genotyping
pin4-3 FW	At2g01420	CAACGCCGTTAAATATGG	Genotyping
pin4-3 RV	At2g01420	TGCAGCAAAACCCACACTTTTACTTC	Genotyping
pin7-2 FW	At1g23080	TTTACTTGAACAATGGCCACAC	Genotyping
pin7-2 RV	At1g23080	GGTAAAGGAAGTGCCTAACGG	Genotyping
aux1-21 FW	At2g38120	TGCTACCAAAGCACTACTACTAC	Genotyping
aux1-21 RV	At2g38120	GAAATGGCTGAAACCAACTCAA	Genotyping

lax1 FW	At5g01240	ATATGGTTGCAGGTGGCACA	Genotyping
lax1 RV	At5g01240	GTAACCGGCAAAAGCTGCA	Genotyping
lax2 FW	At2g21050	ATGGAGAACGGTGAGAAAGCAGC	Genotyping
lax2 RV	At2g21050	CGCAGAAGGCAGCGTTAGCG	Genotyping
lax3 FW	At1g77690	TACTTCACCGGAGCCACCA	Genotyping
PP2A-3 FW	At2g42500	ACGTGGCCAAAATGATGCAA	qRT-PCR
PP2A-3 RV	At2g42500	TCATGTTCTCCACAACCGCT	qRT-PCR
YUCCA1 FW	At4g32540	TTAGCTTAGACCTCGTCGGACAT	qRT-PCR
YUCCA1 RV	At4g32540	TGGCAACACATGAACGGTGT	qRT-PCR
YUCCA2 FW	At4g13260	TGTTTTGGACGTTGGCACTCT	qRT-PCR
YUCCA2 RV	At4g13260	TACCCGTTTCAACTCCGGATA	qRT-PCR
YUCCA3 FW	At1g04610	CCTACGCAGCCAACTTTGACA	qRT-PCR
YUCCA3 RV	At1g04610	GCCCGAACGTCTCATCATATTT	qRT-PCR
YUCCA4 FW	At5g11320	TCTAGCCGTAGCGGCTTGTTT	qRT-PCR
YUCCA4 RV	At5g11320	AAACAATCGGTTCTCTCGAGGA	qRT-PCR
YUCCA5 FW	At5g43890	TGTCCAGTCTGCTCGATACGA	qRT-PCR
YUCCA5 RV	At5g43890	CACCGGCAGATATATTCCATCTC	qRT-PCR
YUCCA6 FW	At5g25620	CGGTATGGAGGTTTGTTTGGAT	qRT-PCR
YUCCA6 RV	At5g25620	ATGGACAGCCCAAAAGTTGAAG	qRT-PCR
YUCCA7 FW	At2g33230	CCCGGAGTATCCAACGAAGTAC	qRT-PCR
YUCCA7 RV	At2g33230	TGATTGGACCGTCTCATTGAAC	qRT-PCR
YUCCA8 FW	At4g28720	TGACCTAGCAAACCATTTCGCT	qRT-PCR
YUCCA8 RV	At4g28720	CATCTTCATTGCAAGCTCAAACG	qRT-PCR
YUCCA9 FW	At1g04180	TTCTCAGAGCGGCGATGTGT	qRT-PCR
YUCCA9 RV	At1g04180	CACAACGAATGGGACTCCTTGA	qRT-PCR
YUCCA10 FW	At1g48910	AAGTATGCTCCAGTGGCGATG	qRT-PCR
YUCCA10 RV	At1g48910	GGAAGAGTCCGTACTTGGAGAGATC	qRT-PCR
YUCCA11 FW	At1g21430	GACGAATACGCCACACGTTTC	qRT-PCR
YUCCA11 RV	At1g21430	ACCATCTTTGAAGTACGCGGA	qRT-PCR
TAA1 FW	At1g70560	GCAGAGCTGGAGAGCGTTGTG	qRT-PCR
TAA1 RV	At1g70560	CTTCATGTTGGCGAGTCTCTCGAG	qRT-PCR
TAR1 FW	At1g23320	CAGGAAGGCTCCTCAGACATTGC	qRT-PCR
TAR1 RV	At1g23320	CGCTGGTCAGAGTTATGAGACACC	qRT-PCR
TAR2 FW	At4g24670	GGTTGTGTCAGACAGTTGTGGG	qRT-PCR
TAR2 RV	At4g24670	GGTTGTGGCTCAAAGACCCTGC	qRT-PCR
TIP41 FW	Solyc10g049850	ATGGAGTTTTTGAGTCTTCTGC	qRT-PCR
TIP41 RV	Solyc10g049850	GCTGCGTTTCTGGCTTAGG	qRT-PCR
ToFZY1 FW	Solyc06g065630	GTACTCGACGTTGGAGCATTATC	qRT-PCR
ToFZY1 RV	Solyc06g065630	TGAAGAAATCATTTCCCTTAAACC	qRT-PCR
ToFZY2 FW	Solyc08g068160	AGGAATGGAGGTGTGTTTGG	qRT-PCR
ToFZY2 RV	Solyc08g068160	GGGACGTGTCACCGAGTAA	qRT-PCR

Table S4: CAPS / PCR-RFLP markers for genotyping.

PCR fragment	CAPS / RFLP	Wild-type product	Mutant product
phyA-201	HinfI	±190 bp	241 bp
phyB-5	BsaBI	666 bp	±250 bp
phyA-1	EcoNI	236 bp	±180 bp
phyB1-1	HinfI	±100 bp	193 bp
phyB2-1	FokI	±300 bp	536 bp

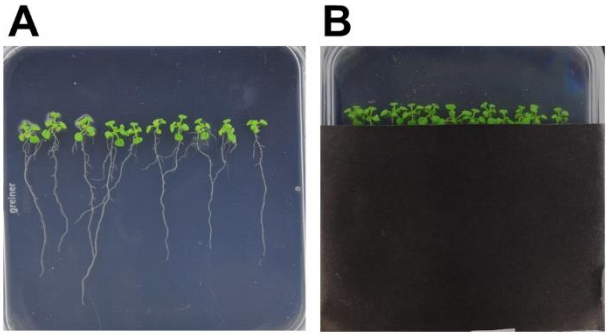

Figure S1: LGR and DGR growth conditions.

A. Arabidopsis **s**eedlings grown in the light-grown root (LGR) condition, where the shoots and roots are exposed to light. **B.** Arabidopsis seedlings grown in the dark-grown (DGR) condition, where only the shoots are exposed to light.

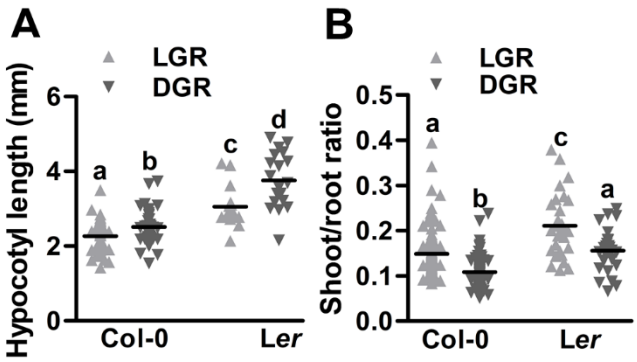

Figure S2: Arabidopsis DGR seedlings show a reduced shoot/root ratio despite their longer hypocotyls.

A. Quantification of the hypocotyl length of 7-day-old Arabidopsis seedings of ecotypes Columbia (Col-0) and Landsberg *erecta* (L*er*) that were grown in light-grown roots (LGR) or dark-grown roots (DGR) conditions. **B.** Quantification of the shoot/root ratio of 7-day-old Col-0 and L*er* seedlings that were grown in LGR or DGR conditions. Hypocotyl lengths or shoot/root ratios were compared using a one-way ANOVA followed by a Tukey's test (letters **a**, **b**, **c**, and **d** indicate statistically different values, $p<0.05$). In the graphs, the horizontal line indicates the mean, error bars indicating standard error of the mean are not visible due to limited variation, and triangles indicate values of biologically independent observations (n=30). Similar results were obtained from three independent experiments.

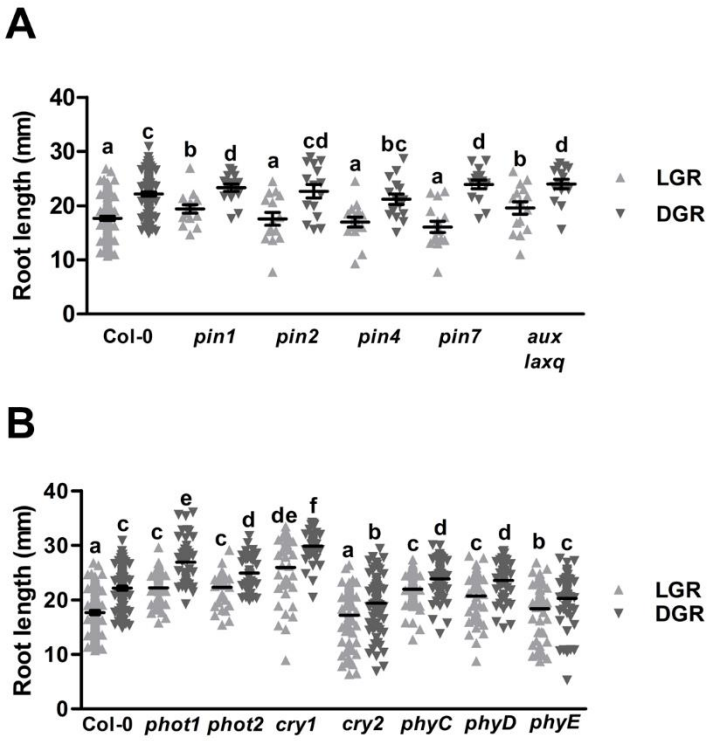

Figure S3: Seedling roots of several Arabidopsis photoreceptor mutants are shorter in light-grown conditions.

A. Quantification of the primary root length of 7-day-old Arabidopsis pin-formed (*pin*) and auxin1/like-aux1 (*aux/lax*) mutants that were grown in LGR or DGR conditions. **B.** Quantification of the primary root length of 7-day-old Arabidopsis phototropin (*phot*), cryptochrome (*cry*) or phytochrome (*phy*) single mutants that were grown in LGR or DGR conditions. Primary root lengths were compared using a one-way ANOVA followed by a Tukey's test (letters **a**, **b**, **c**, **d**, **e**, and **f** indicate statistically different values, $p<0.05$). In the graphs, the horizontal line indicates the mean, error bars represent standard error of the mean (for some not visible due to limited variation), and triangles indicate values of biologically independent observations (n=30). Similar results were obtained from three independent experiments.